Antigen delivery targeted to tumor-associated macrophages overcomes tumor immune resistance

Authors: Daisuke Muraoka[1,2,3], Naohiro Seo[1,4], Tae Hayashi[1], Yoshiro Tahara[4,5,6], Keisuke Fujii[1], Isao Tawara[7], Yoshihiro Miyahara[1], Kana Okamori[1], Hideo Yagita[8], Seiya Imoto[9], Rui Yamaguchi[10], Mitsuhiro Komura[9], Satoru Miyano[10], Masahiro Goto[6], Shin-ichi Sawada[4,5], Akira Asai[3], Hiroaki Ikeda[2], Kazunari Akiyoshi[4,5], Naozumi Harada[1,4,11], and Hiroshi Shiku[1,4]

Affiliations:

[1]Department of Immuno-Gene Therapy, Mie University Graduate School of Medicine, Mie 514-8507, Japan. [2]Department of Oncology, Nagasaki University Graduate School of Biomedical Sciences 852-8523, Japan. [3]Center for Drug Discovery, Graduate School of Pharmaceutical Sciences, University of Shizuoka, Shizuoka 422-8526, Japan. [4]ERATO Akiyoshi Bio-Nanotransporter Project, Japan Science and Technology Agency (JST), Tokyo 102-0076, Japan. [5]Department of Polymer Chemistry, Kyoto University Graduate School of Engineering, Kyoto 615-8510, Japan. [6]Department of Applied Chemistry, Graduate School of Engineering, Kyushu University, 744 Motooka, Nishi-ku, Fukuoka 819-0395, Japan. [7]Department of Hematology and Oncology, Mie University Graduate School of Medicine, Mie 514-8507, Japan. [8]Department of Immunology, Juntendo University School of Medicine, Tokyo 113-8421, Japan. [9]Division of Health Medical Data Science, Health Intelligence Center, Institute of Medical Science, University of Tokyo, Tokyo 108-8639, Japan. [10]Laboratory of DNA Information Analysis, Human Genome Center, Institute of Medical Science, University of Tokyo, Tokyo 108-8639, Japan. [11]United Immunity, Co., Ltd., Mie 514-8507, Japan.

Supplemental Information:

Supplemental Figure 1. Blockade of each checkpoint molecule brings weak or no therapeutic effect in the tested murine tumor models.

Supplemental Figure 2. CMS5a tumor lacks highly immunogenic antigens.

Supplemental Figure 3. Expression of differentiation and activation markers on TILs does not differ between the immune-sensitive and resistant tumors.

Supplemental Figure 4. Spontaneous tumor-specific $CD8^+$ T cell responses are weak or undetectable in untreated tumors.

Supplemental Figure 5. TAMs from CT26 tumor present tumor antigen to specific $CD8^+$ T cells.

Supplemental Figure 6. TAMs of resistant CMS5a tumor have potential for antigen presentation.

Supplemental Figure 7. Physical characteristics of the CHP:LPA nanoparticle.

Supplemental Figure 8. Macrophages from various organs except tumor do not present vaccine antigen after intravenous administration of CHP:LPA and CpG ODN.

Supplemental Figure 9. No toxicological changes related to the administration of CHP:LPA are observed in tumor-bearing mice. Administration of CHP:LPA has no toxicity.

Supplemental Figure 10. Intravenous injection of the CHP:LPA does not induce specific $CD8^+$ T cell response in CMS5a tumor- bearing mice even if combined with checkpoint inhibitors.

Supplemental Figure 11. CpG ODN supports TAM activation.

Supplemental Figure 12. Synergistic effect of CHP:LPA and ACT was also observed in the presence of poly-IC RNA instead of CpG ODN.

Supplemental Figure 13. Intravenously injected clodronate liposome efficiently depletes macrophages in the tumor and the spleen but not in the lymph node.

Supplemental Figure 14. Intravenous injection of the CHP:LPA with CpG ODN suppresses the expression of immune checkpoint molecules on TILs in B16 melanoma-bearing mice.

Supplemental Figure 15. T-bet expression increases in tumor-specific T cells TILs after the intravenous injection of the CHP:LPA and CpG ODN.

Supplemental Table 1. Tested peptides of neoepitopes predicted in CT26 cells.

Supplemental Table 2. Tested peptides of neoepitopes predicted in CMS7 cells.

Supplemental Table 3. Tested peptides of neoepitopes predicted in CMS5a cells.

Supplemental Table 4. Number of non-synonymous SNVs in transcripts in the tested murine tumors.

Supplemental Table 5. Comparative gene expression analysis of transcription factors associated with M1 and M2 macrophages.

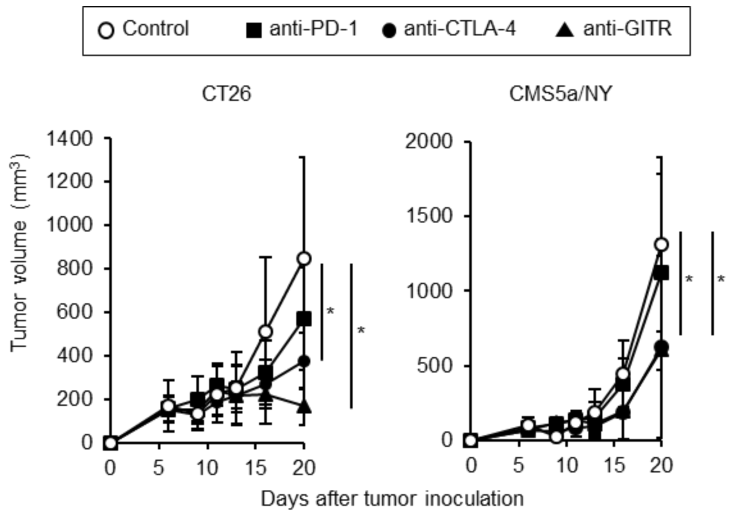

Supplemental Figure 1. Blockade of each checkpoint molecule brings weak or no therapeutic effect in the tested murine tumor models. Murine tumor cell lines CT26 and CMS5a/NY were subcutaneously inoculated into BALB/c mice. Each checkpoint inhibitor (anti-PD-1, anti-CTLA-4, or anti-GITR) or isotype control antibody was intraperitoneally injected on days 7, 9, and 11. The tumor size was then monitored (n = 6 to 8 per group). p-values were determined by Steel-Dwass test. *, $p < 0.05$. These experiments were repeated twice with similar results.

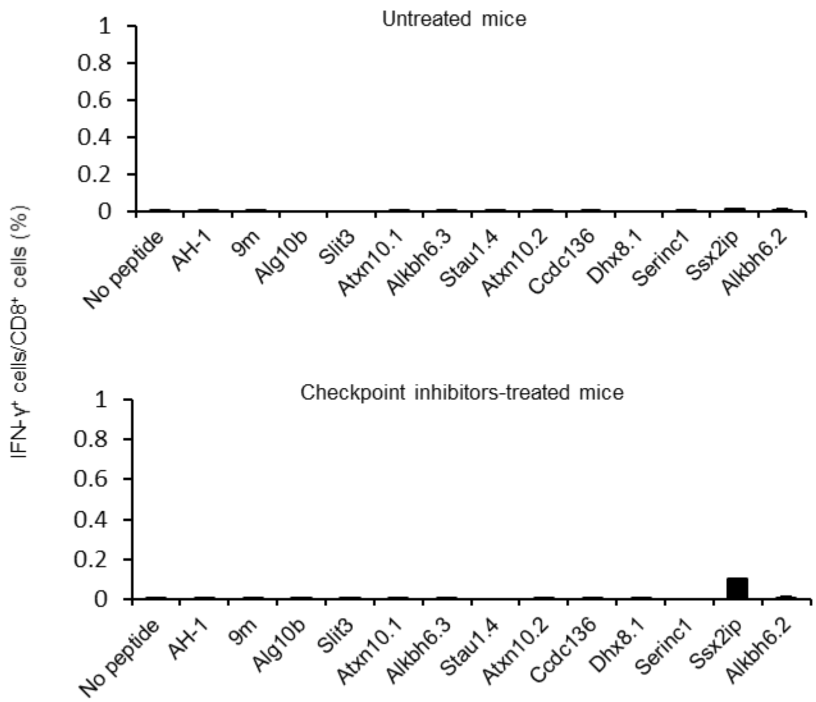

Supplemental Figure 2. CMS5a tumor lacks highly immunogenic antigens. CMS5a cells were subcutaneously inoculated into BALB/c mice. A mixture of anti-PD-1, anti-CTLA-4, and anti-GITR antibody was intraperitoneally injected on days 7, 9, and 11. Seven days after the last administration, splenocytes were isolated and re-stimulated with epitope peptides of indicated, reported neoantigens (40). AH-1 epitope peptide of endogenous murine leukemia provirus antigen reported in CT26 tumor was included as a negative control. The frequency of activated specific $CD8^+$ T cells was quantified by using intracellular IFN-γ staining followed by flow cytometry (three mice per group). These experiments were repeated at least twice with similar results.

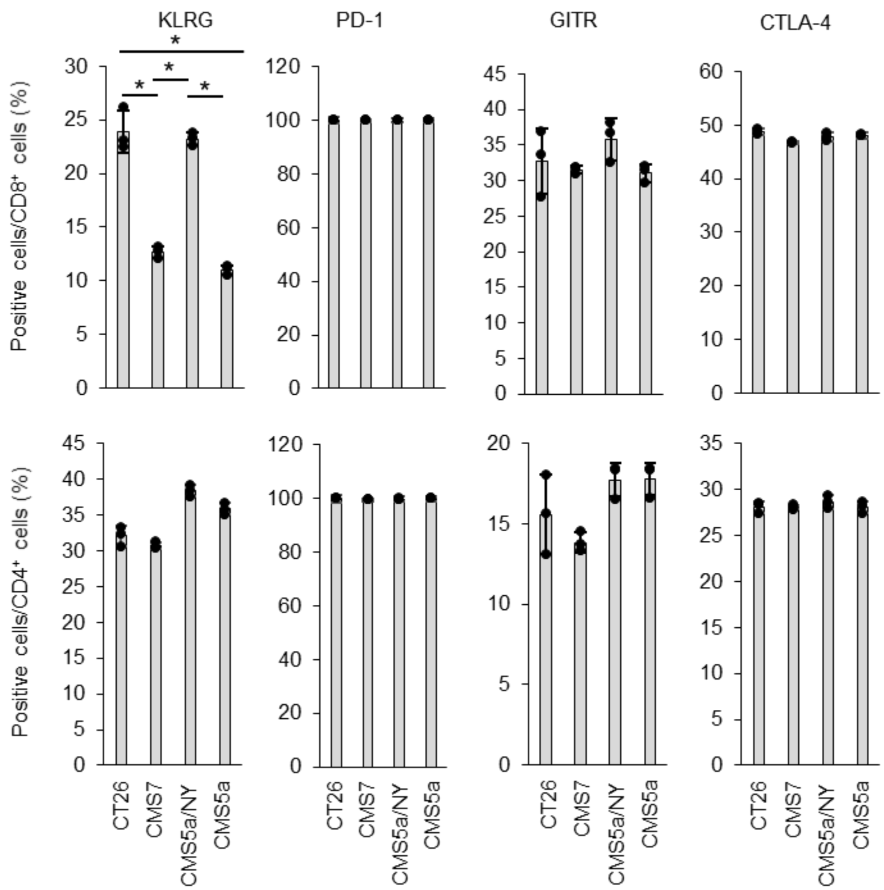

Supplemental Figure 3. Expression of differentiation and activation markers on TILs does not differ between the immune-sensitive and resistant tumors. CT26, CMS7, CMS5a/NY, or CMS5a cells were subcutaneously inoculated into BALB/c mice. Checkpoint inhibitors including anti-PD-1 (200 μg/mouse), anti-CTLA-4 (100 μg/mouse), and anti-GITR (200 μg/mouse) antibodies were intraperitoneally injected on days 7, 9, and 11. Expression of KLRG, PD-1, GITR and CTLA-4 on $CD8^+$ or $CD4^+$ TILs was determined by flow cytometry at 7 days after last treatment. Data are the mean ± SD of four tumors per group. p-values were determined by a two-factor factorial ANOVA followed by Tukey–Kramer post hoc analysis. *, $p < 0.05$. These experiments were repeated twice with similar results.

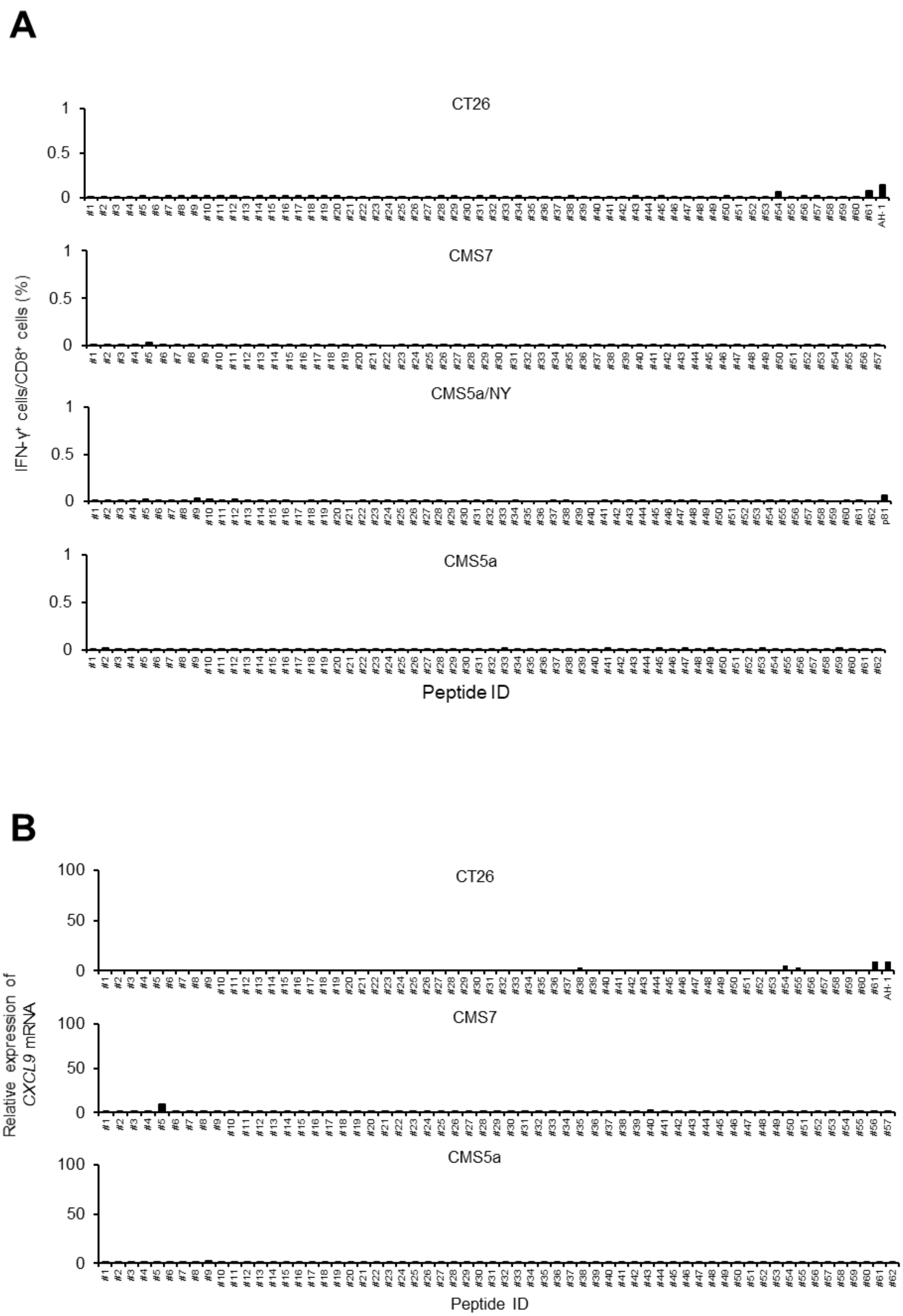
A
CT26
CMS7
CMS5a/NY
CMS5a
IFN-γ⁺ cells/CD8⁺ cells (%)
Peptide ID
B
CT26
CMS7
CMS5a
Relative expression of CXCL9 mRNA
Peptide ID

Supplemental Figure 4. Spontaneous tumor-specific CD8$^+$ T cell responses are weak or undetectable in untreated tumors. Splenocytes were isolated from BALB/c mice bearing CT26, CMS7, CMS5a/NY, or CMS5a tumors on day 18, and were re-stimulated with peptides of predicted neoantigens. In the CT26 and CMS5a/NY tumors, AH-1 and NY-ESO-1 p81 epitopes were also tested, respectively. The frequency of activated specific CD8$^+$ T cells was quantified by using (A) intracellular IFN-γ staining followed by flow cytometry (two mice per group) or (B) quantitative reverse transcription PCR for *CXCL9* mRNA. The level of *CXCL9* mRNA expression is shown as fold increase compared with unstimulated control. These experiments were repeated at least twice with similar results.

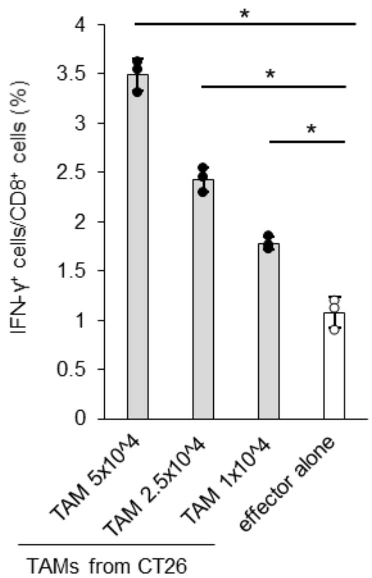

Supplemental Figure 5. TAMs from CT26 tumor present tumor antigen to specific CD8⁺ T cells. CT26 cells were subcutaneously inoculated into BALB/c mice. TAMs were sorted from the CT26 tumor-bearing mice on day 7 and were co-cultured as antigen-presenting cells with AH-1-specific TCR gene-transduced $CD8^+$ T cells as responder cells for 16 h. IFN-γ production in $CD8^+$ T cells upon antigen stimulation was detected by using flow cytometry (n = 3 per group). p-values were determined by Dunnett test. The data are the mean ± SD. *, $p < 0.05$. These experiments were repeated twice with similar results.

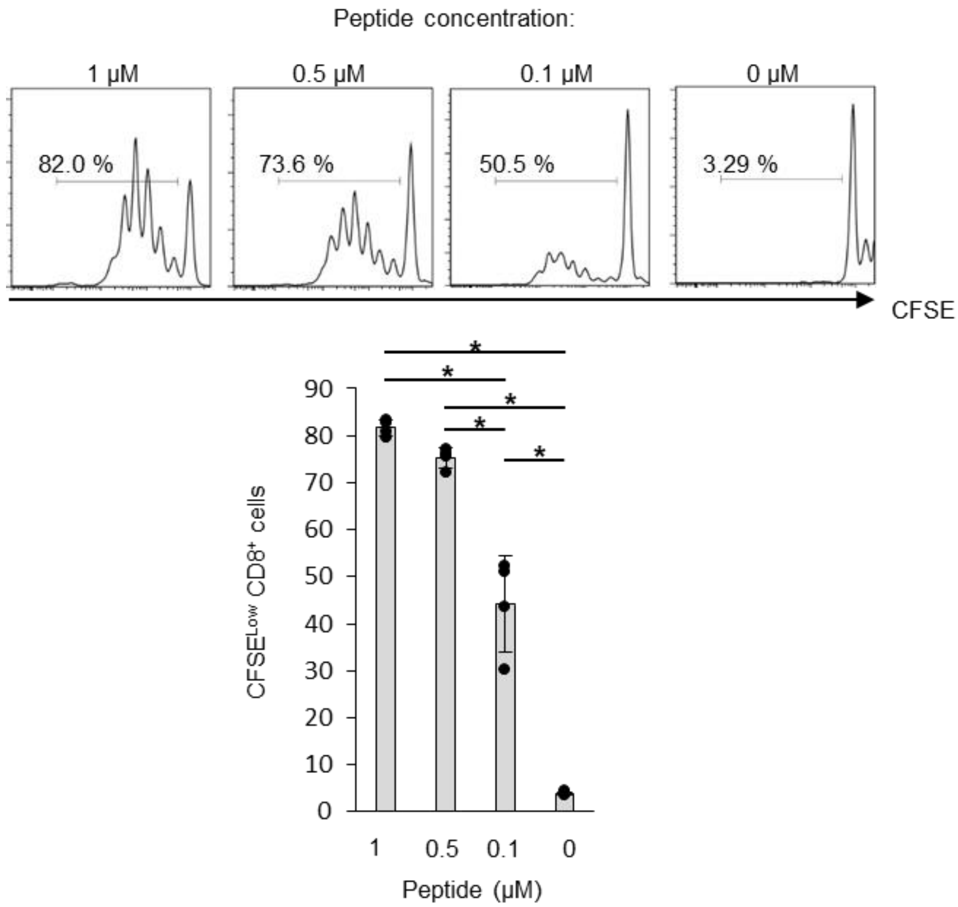

Supplemental Figure 6. TAMs of resistant CMS5a tumor have potential for antigen presentation. CD11b$^+$ TAMs were isolated from CMS5a tumors grown in BALB/c mice on day 7, and pulsed with 9m peptide at 0, 0.1, 0.5, or 1 μM in the presence of CpG ODN. These cells were then co-cultured as antigen-presenting cells with 9m-specific DUC18 CD8$^+$ T cells for 72 h in vitro. Proliferation of DUC18 CD8$^+$ T cells was measured using CFSE dilution assay (n = 3 per group). The histograms show representative data, and the numbers shown in histograms indicate the percentages of proliferating cells. The data in bar graph are mean ± SD. p-values were determined by a two-factor factorial ANOVA followed by Tukey–Kramer post hoc analysis. *, $p < 0.05$. These experiments were repeated at least twice with similar results.

A

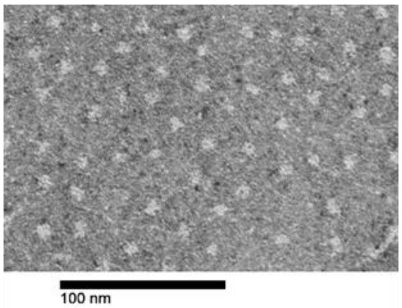

B

	Size	Z potential
CHP: LPA	38.6 ± 1.0 nm	−3.3 ± 0.5 mV

n=5

Supplemental Figure 7. Physical characteristics of the CHP:LPA nanoparticle

(**A**) Transmission electron microscopy (TEM) of the CHP:LPA complex. (**B**) Dynamic light scattering (DLS) analysis and ζ-potential measurement of the CHP:LPA complex. The observed apparent particle size differs between TEM and DLS analyses (about 10 and 39 nm, respectively). It is highly likely that in TEM analysis, the evacuated condition would cause dehydration of CHP nanogel, leading to the decreased particle size. These experiments were repeated twice with similar results.

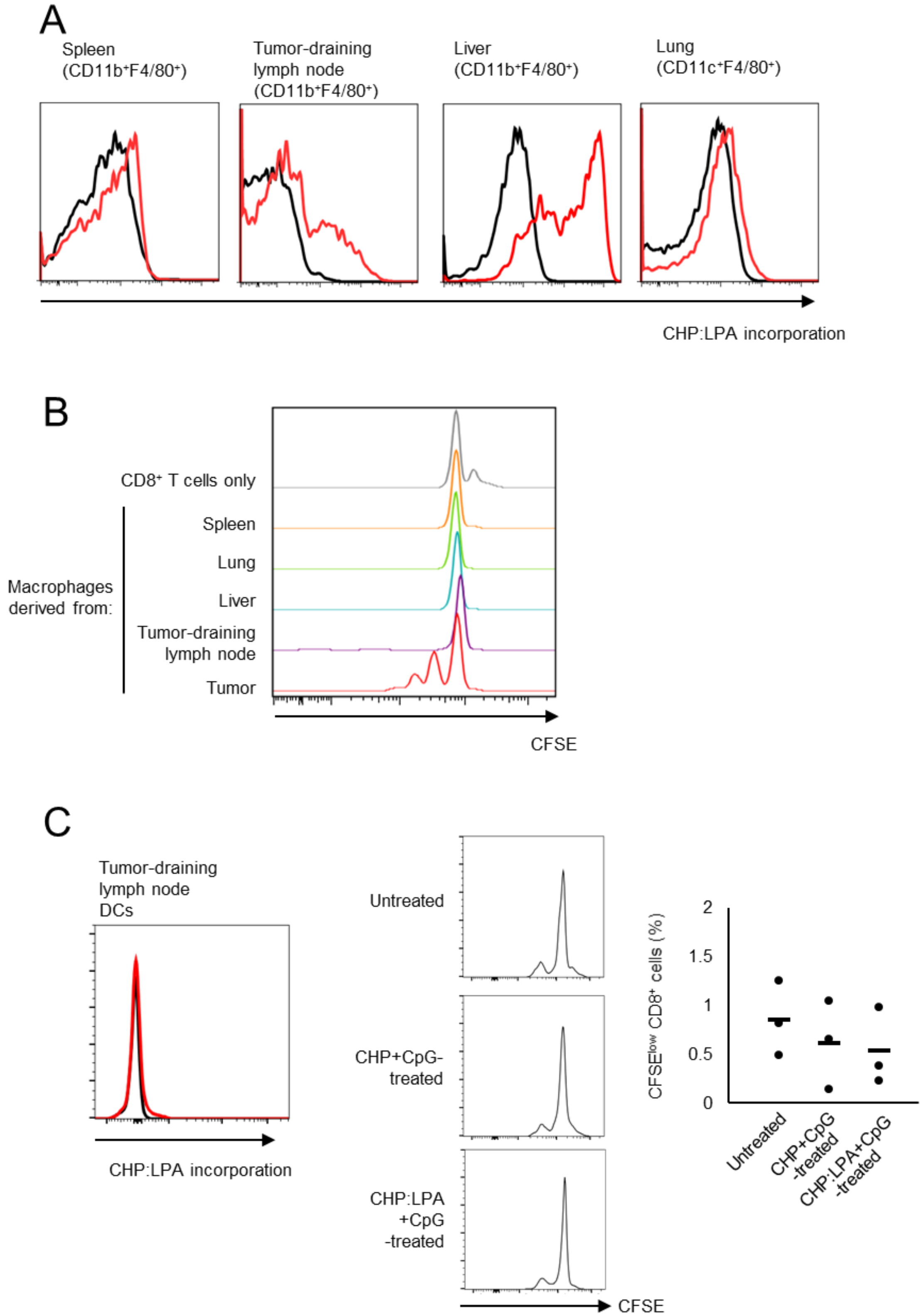
A
Spleen
(CD11b+F4/80+)
Tumor-draining
lymph node
(CD11b+F4/80+)
Liver
(CD11b+F4/80+)
Lung
(CD11c+F4/80+)
CHP:LPA incorporation
B
CD8+ T cells only
Spleen
Lung
Liver
Tumor-draining
lymph node
Tumor
Macrophages
derived from:
CFSE
C
Tumor-draining
lymph node
DCs
CHP:LPA incorporation
Untreated
CHP+CpG-
treated
CHP:LPA
+CpG
-treated
CFSE
CFSElow CD8+ cells (%)
2
1.5
1
0.5
0
Untreated
CHP+CpG
-treated
CHP:LPA+CpG
-treated

Supplemental Figure 8. Macrophages from various organs except tumor do not present vaccine antigen after intravenous administration of CHP:LPA and CpG ODN. (**A**) Incorporation of intravenously injected CHP:LPA complex into macrophages in various organs. BALB/c mice were intravenously injected with rhodamine-CHP:LPA, and 18 h later, the uptake of CHP:LPA in macrophages in each organ was evaluated using flow cytometry. (**B**) The complex of CHP and LPA containing 9m epitope was intravenously injected with CpG ODN into BALB/c mice. Eighteen hours later, CD11c$^+$ cells in the lung and CD11b$^+$ cells in other indicated organs and tumor were isolated as macrophages. These cells were co-cultured as antigen-presenting cells with 9m-specific DUC18 CD8$^+$ T cells for 72 h in vitro. Proliferation of T cells was measured using CFSE dilution assay. (**C**) The complex of CHP and LPA containing 9m epitope was intravenously injected with CpG ODN into BALB/c mice. Eighteen hours later, CD11c$^+$ cells in the tumor-draining lymph node were isolated as dendritic cells (DCs). These cells were co-cultured as antigen-presenting cells with 9m-specific DUC18 CD8$^+$ T cells for 72 h in vitro. Proliferation of T cells was measured using CFSE dilution assay. These experiments were repeated twice with similar results.

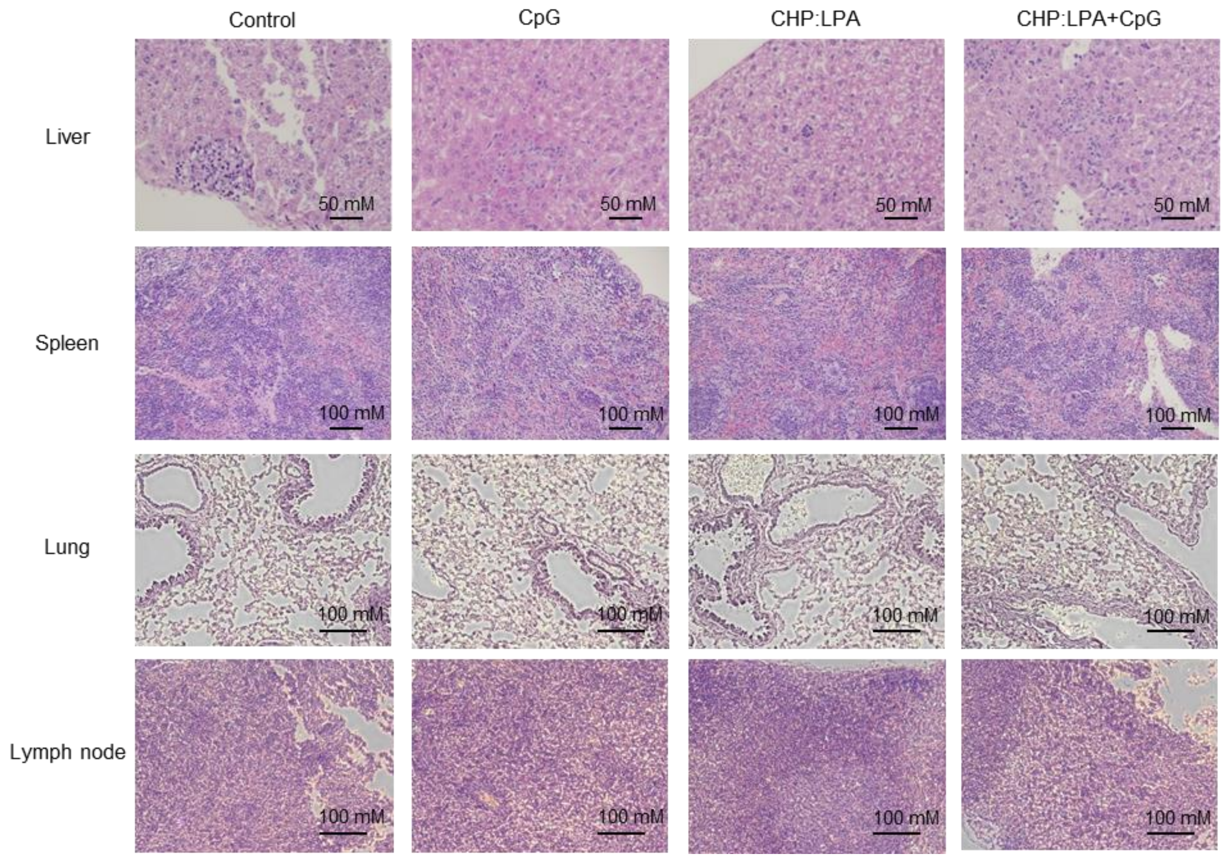

Supplemental Figure 9. No toxicological changes related to the administration of CHP:LPA are observed in tumor-bearing mice. CMS5a cells were subcutaneously inoculated into BALB/c mice. The complex of CHP with 9m epitope-containing LPA (50 μg) was intravenously injected with CpG ODN (50 μg) into the same mice on days 7 and 11. The liver, spleen, lung and lymph node were collected and embedded into paraffin. Sections of these tissues were then subjected to H&E staining.

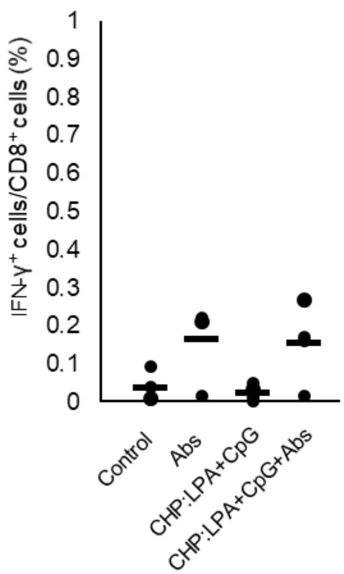

Supplemental Figure 10. Intravenous injection of the CHP:LPA does not induce specific $CD8^+$ T cell response in CMS5a tumor-bearing mice even if combined with checkpoint inhibitors. CMS5a cells were subcutaneously inoculated into BALB/c mice. The complex of CHP with 9m epitope-containing LPA (50 μg) was intravenously injected with CpG ODN (50 μg) into the same mice on days 7 and 11. (A) Checkpoint inhibitors including anti-PD-1 (200 μg/mouse), anti-CTLA-4 (100 μg/mouse), and anti-GITR (200 μg/mouse) antibodies or isotype antibodies were intraperitoneally injected on days 7, 9, and 11. Seven days after the last administration, splenocytes were isolated and re-stimulated with 9m epitope peptide. The frequency of stimulated $CD8^+$ T cells was quantified by intracellular IFN-γ staining (n = 3 per group). p-values were determined by a two-factor factorial ANOVA followed by Tukey–Kramer post hoc analysis. *, $p < 0.05$. These experiments were repeated twice with similar results.

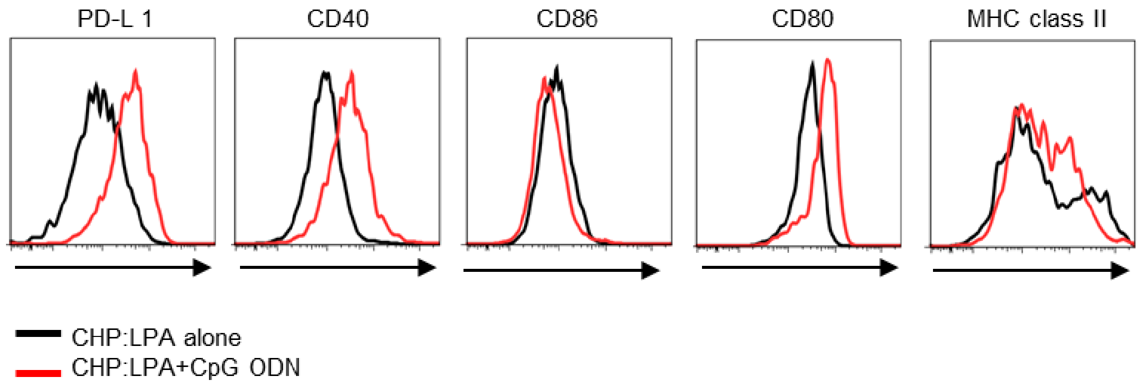

Supplemental Figure 11. CpG ODN supports TAM activation. CMS5a tumors were subcutaneously inoculated into BALB/c mice. Seven days later, CHP:LPA with or without CpG ODN were intravenously injected into the mice. One day after injection, tumors were collected, and TAMs were tested for the expression of PD-L1, CD40, CD86, CD80, and MHC class II by flow cytometry. These experiments were repeated twice with similar results.

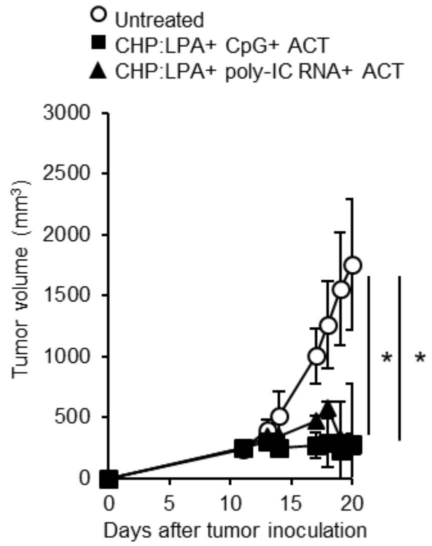

Supplemental Figure 12. Synergistic effect of CHP:LPA and ACT was also observed in the presence of poly-IC RNA instead of CpG ODN. The complex of CHP with 9m epitope-containing LPA was intravenously injected with poly-IC RNA to CMS5a tumor-bearing BALB/c mice on days 7 and 11. Naïve $CD8^+$ cells isolated from DUC18 mice were infused into the same mice on days 8 and 12. Tumor size was then monitored (n = 6 to 8 per group). p-values were determined by Steel-Dwass test. *, $p < 0.05$. The data are the mean ± SD. These experiments were repeated twice with similar results.

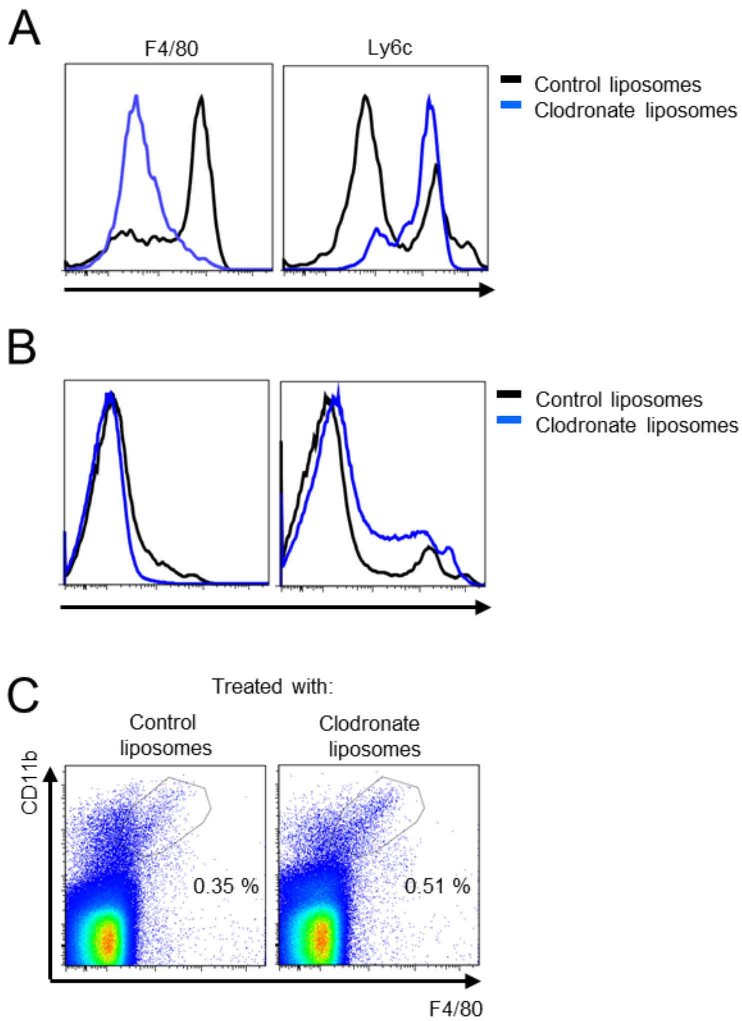

Supplemental Figure 13. Intravenously injected clodronate liposome efficiently depletes macrophages in the tumor and the spleen but not in the lymph node. CMS5a tumors were subcutaneously inoculated into BALB/c mice. Seven days after inoculation, clodronate liposomes or control liposomes were intravenously injected into the mice. One day after treatment, the depletion of macrophages was confirmed in the tumor (**A**), the spleen (**B**) and the inguinal lymph node (**C**) by using flow cytometry. These experiments were repeated twice with similar results.

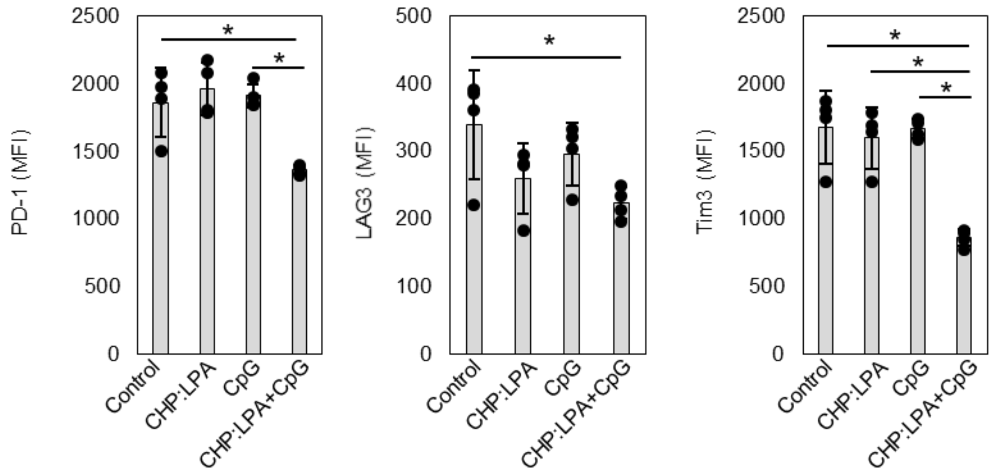

Supplemental Figure 14. Intravenous injection of the CHP:LPA with CpG ODN suppress the expression of immune checkpoint molecules on TILs in B16 melanoma-bearing mice.

The complex of CHP with gp100 epitope-containing LPA (50 μg) was intravenously injected with CpG ODN (50 μg) into B16 tumor-bearing C57BL/6 mice (n = 4 per group) on day 7. Expression of PD-1, LAG3, and Tim3 on $CD8^+$ TILs was determined by flow cytometry on day 10. p-values were determined by a two-factor factorial ANOVA followed by Tukey–Kramer post hoc analysis. The data are the mean ± SD. *, $p < 0.05$. These experiments were repeated twice with similar results.

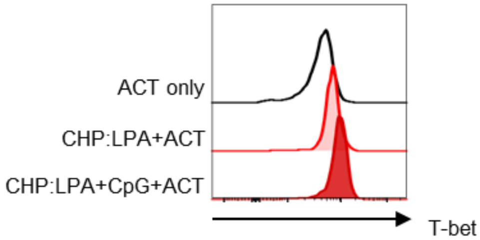

Supplemental Figure 15. T-bet expression increases in tumor-specific TILs after intravenous injection of the CHP:LPA and CpG ODN. The complex of CHP with 9m epitope-containing LPA (50 μg) was intravenously injected with CpG ODN (50 μg) into CMS5a tumor-bearing BALB/c mice (n = 2 per group) on day 7. Naïve $CD8^+$ cells isolated from DUC18/CD90.1 mice were infused into the same mice on day 8. The tumors were removed from the mice on day 11, and the expression of T-bet in $CD90.1^+CD8^+$ T cells in the tumors was determined by flow cytometry. These experiments were repeated three times with similar results.

Supplemental Table 1. Tested peptides of neoepitopes predicted in CT26 cells.

Peptide ID	Peptide sequence	IEDB analysis			Substitution (wild type, amino acid number, mutation)	Gene
		MHC allele	Percentile rank	ANN IC50		
No. 1	PPQNMFEF	H-2-Ld	0.2	51	G, 1814, E	*Phf3*
No. 2	FPPQNMFEF	H-2-Dd	0.2	1,131	G, 1814, E	*Phf3*
No. 3	FPPQNMFE	H-2-Dd	0.5	3,888	G, 1814, E	*Phf3*
No. 4	LPCDLHLF	H-2-Ld	0.5	515	P, 409, L	*Zfp451*
No. 5	SNTLSKSAI	H-2-Kd	0.2	644	E, 344, K	*Ifi203*
No. 6	SENRSLFFL	H-2-Ld	0.45	1,054	S, 257, F	*Cr1l*
No. 7	LYYESDEFTV	H-2-Kd	0.55	2,185	D, 376, Y	*Suv39h2*
No. 8	NAPERGFSL	H-2-Dd	0.2	1,543	D, 178, N	*Mettl15*
No. 9	TGPYVMMI	H-2-Dd	0.2	688	A, 986, T	*Trpm7*
No. 10	SYTSYIMAI	H-2-Kd	0.3	28	T, 425, I	*Slc20a1*
No. 11	SYIMAICGM	H-2-Kd	0.4	146	T, 425, I	*Slc20a1*
No. 12	FPSPLGGI	H-2-Ld	0.5	430	S, 485, F	*Xrn2*
No. 13	GFPSPLGGI	H-2-Dd	0.5	3,806	S, 485, F	*Xrn2*
No. 14	SYAEKSDEI	H-2-Kd	0.6	85	P, 7, S	*2310003C23Rik*

No. 15	KPLSKTAF	H-2-Ld	0.6	946	L, 485, F	*Eif2a*
No. 16	AGPDEKEE	H-2-Dd	0.3	2,832	G, 486, E	*Pdzk1*
No. 17	AGPDEKEET	H-2-Dd	0.5	2,763	G, 486, E	*Pdzk1*
No. 18	GPPGGFQEF	H-2-Dd	0.3	2,149	L, 371, F	*Fubp1*
No. 19	PGGFQEFNF	H-2-Dd	0.4	3,347	L, 371, F	*Fubp1*
No. 20	SYETLKKSL	H-2-Kd	0.3	21	A, 821, T	*Haus6*
No. 21	HHTMMVQAI	H-2-Kd	0.4	126	V, 971, M	*Mtor*
No. 22	FPPTQSTW	H-2-Dd	0.3	2,319	A, 1916, T	*Ankrd17*
No. 23	NYLAPRGL	H-2-Kd	0.4	566	T, 565, P	*Chfr*
No. 24	NGGIYEGIF	H-2-Dd	0.6	2,934	V, 263, I	*Atxn2*
No. 25	NPPRTSVL	H-2-Dd	0.2	1,116	N, 384, S	*Por*
No. 26	TNPPRTSVLY	H-2-Dd	0.2	3,840	N, 384, S	*Por*
No. 27	VMPGLAVL	H-2-Dd	0.4	3,115	V, 197, M	*Gpr146*
No. 28	CQIAMVHYI	H-2-Kd	0.5	294	Y, 282, C	*Impdh1*
No. 29	KGPKRDEQC	H-2-Dd	0.4	1,101	Y, 529, C	*4933424B01Rik*
No. 30	TPSGPQSF	H-2-Ld	0.6	1,069	S, 732, F	*Zfp865*
No. 31	SGPSYATY	H-2-Dd	0.1	443	I, 522, T	*E2f8*
No. 32	SGPSYATYL	H-2-Dd	0.4	362	I, 522, T	*E2f8*
No. 33	TYLQPAQA	H-2-Kd	0.55	2,240	I, 522, T	*E2f8*
No. 34	GQPVSSLRF	H-2-Dd	0.5	3,642	G, 900, S	*Pcf11*
No. 35	QPVSSLRF	H-2-Ld	0.6	833	G, 900, S	*Pcf11*

No. 36	LPVAGPEM	H-2-Ld	0.1	15	A, 820, P	*Mvp*
No. 37	TPASTLEL	H-2-Ld	0.6	952	P, 255, L	*Fam53b*
No. 38	AMPQAASL	H-2-Dd	0.4	3,101	V, 510, A	*Prmt7*
No. 39	INQNRFFM	H-2-Ld	0.3	201	L, 610, F	*Cwf19l2*
No. 40	YPGPGNYF	H-2-Ld	0.1	29	H, 145, Y	*Tdg*
No. 41	PGPGNYFW	H-2-Dd	0.2	1,085	H, 145, Y	*Tdg*
No. 42	PGPGNYFWK	H-2-Dd	0.6	3,175	H, 145, Y	*Tdg*
No. 43	LYLRILMPI	H-2-Kd	0.4	80	A, 148, P	*Xpot*
No. 44	SFQSLEESI	H-2-Kd	0.3	23	M, 703, I	*Stat6*
No. 45	IPILEMQF	H-2-Ld	0.4	323	V, 295, M	*Snap47*
No. 46	NYLEFSEDSV	H-2-Kd	0.3	525	S, 287, N	*Fxr2*
No. 47	CSPSRLAW	H-2-Dd	0.3	2,114	R, 679, W	*2010111I01Rik*
No. 48	YPSPSPLL	H-2-Ld	0.3	172	H, 111, Y	*Hnrnpc*
No. 49	EAPRQAEL	H-2-Dd	0.5	3,587	R, 2336, Q	*Chd8*
No. 50	FPSESEFF	H-2-Ld	0.3	141	L, 1008, F	*Chd8*
No. 51	QFPSESEFF	H-2-Dd	0.3	2,464	L, 1008, F	*Chd8*
No. 52	FPIAWHRL	H-2-Ld	0.1	16	C, 751, W	*Mphosph8*
No. 53	VGPSAPDI	H-2-Dd	0.2	1,433	T, 52, I	*Dtx3l*
No. 54	VGPSAPDIY	H-2-Dd	0.6	588	T, 52, I	*Dtx3l*
No. 55	SAPQKRKL	H-2-Dd	0.4	3,383	G, 148, R	*Dscr3*
No. 56	EPQVEPLDF	H-2-Ld	0.45	272	L, 715, F	*Zeb1*

No. 57	FTPTSIKF	H-2-Dd	0.4	2,893	N, 290, T	*Dctn4*
No. 58	AYSYAEQTM	H-2-Kd	0.4	124	N, 242, S	*Rbm4b*
No. 59	SYAEQTMSHL	H-2-Kd	0.6	134	N, 242, S	*Rbm4b*
No. 60	IPQAPENL	H-2-Ld	0.2	48	R, 155, Q	*Il2rg*
No. 61	QAPENLTL	H-2-Dd	0.5	3,892	R, 155, Q	*Il2rg*

Supplemental Table 2. Tested peptides of neoepitopes predicted in CMS7 cells.

Peptide ID	Peptide sequence	IEDB analysis			Substitution (wild type, amino acid number, mutation)	Gene
		MHC allele	Percentile rank	ANN IC50		
No. 1	RGPLNLFETC	H-2-Dd	0.15	2,854	C, 59, F	*Plekhg5*
No. 2	VPPAALRL	H-2-Ld	0.2	101	G, 53, R	*Anapc2*
No. 3	TPLNILAL	H-2-Ld	0.2	64	A, 109, P	*Gba*
No. 4	LPVATVTL	H-2-Ld	0.2	98	G, 40, V	*Il6ra*
No. 5	YAPCRGEF	H-2-Dd	0.2	1,371	R, 731, C	*Snd1*
No. 6	LPACKFQL	H-2-Ld	0.2	95	V, 154, L	*Trappc6a*
No. 7	SPYQPKYGF	H-2-Ld	0.2	47	H, 398, P	*Trim12c*
No. 8	VPAEALSF	H-2-Ld	0.2	98	C, 22, F	*Dnase2a*
No. 9	QYAPAAPSEV	H-2-Kd	0.2	248	S, 89, Y	*2810004N23Rik*
No. 10	CGPLKLLV	H-2-Dd	0.2	1,399	A, 237, V	*Supv3l1*
No. 11	YPNRFLHM	H-2-Ld	0.2	42	R, 1168, P	*Gnptab*
No. 12	IPFCLQSF	H-2-Ld	0.2	44	C, 220, F	*Gls2*
No. 13	LYLPMVQSV	H-2-Kd	0.2	23	A, 75, V	*Dazap2*
No. 14	PYSSPSPTAV	H-2-Kd	0.25	332	G, 1009, V	*Ncoa1*

No. 15	EPPDHLTI	H-2-Dd	0.3	2,660	H, 1384, P	*Cep170*
No. 16	RPAPKSFL	H-2-Ld	0.3	119	T, 325, P	*Samhd1*
No. 17	RGPLNLFE	H-2-Dd	0.3	2,340	C, 59, F	*Plekhg5*
No. 18	RGPLNLFET	H-2-Dd	0.3	3,519	C, 59, F	*Plekhg5*
No. 19	EPKQYFDL	H-2-Ld	0.3	203	Q, 1113, L	*Tjp1*
No. 20	DSPYQPKY	H-2-Dd	0.3	2,865	H, 398, P	*Trim12c*
No. 21	SYYLSAGMV	H-2-Kd	0.3	53	R, 115, S	*Slc37a2*
No. 22	MPLEQWWL	H-2-Ld	0.3	135	R, 737, L	*Pfkl*
No. 23	KIPFCLQSF	H-2-Dd	0.3	2,320	C, 220, F	*Gls2*
No. 24	ISPGEEMQF	H-2-Dd	0.3	1,949	L, 641, F	*Timeless*
No. 25	LGPPRSSP	H-2-Dd	0.3	2,125	R, 286, P	*Sh3bp5l*
No. 26	GPPRSSPV	H-2-Dd	0.3	2,437	R, 286, P	*Sh3bp5l*
No. 27	LGPPRSSPV	H-2-Dd	0.3	711	R, 286, P	*Sh3bp5l*
No. 28	KYANRSRNI	H-2-Kd	0.3	52	A, 368, S	*Kif21a*
No. 29	FAPRHSRL	H-2-Dd	0.3	2,431	R, 294, L	*Zfp598*
No. 30	QPPNLIGL	H-2-Dd	0.3	2,728	R, 460, P	*Rbm27*
No. 31	WFQAMANGL	H-2-Kd	0.4	106	R, 211, M	*Strbp*
No. 32	CGPRPRRS	H-2-Dd	0.4	3,179	R, 157, S	*2810432D09Rik*
No. 33	TTPATSTTF	H-2-Dd	0.4	3,370	C, 1340, F	*Cnot1*
No. 34	TYMSSVCWL	H-2-Kd	0.4	22	A, 194, S	*Siae*
No. 35	CGPLKLLVH	H-2-Dd	0.4	1,423	A, 237, V	*Supv3l1*

No. 36	TIMVIVFFL	H-2-Ld	0.4	790	G, 247, V	*H2-DMa*
No. 37	NYRPVALL	H-2-Kd	0.45	1,674	D, 187, N	*Pten*
No. 38	RMPSSAAI	H-2-Dd	0.5	3,632	S, 289, R	*Nfe2l2*
No. 39	PAPKSFLY	H-2-Dd	0.5	3,642	T, 325, P	*Samhd1*
No. 40	VYKWVGSSTA	H-2-Kd	0.5	1,466	A, 102, G	*Exoc1*
No. 41	FPTDCHSI	H-2-Ld	0.5	482	V, 620, I	*Atg2b*
No. 42	LGPEGYSV	H-2-Dd	0.5	3,825	C, 112, Y	*Cyhr1*
No. 43	CYRRASSCSL	H-2-Kd	0.55	164	D, 407, Y	*Ripk2*
No. 44	SYYLSAGMVL	H-2-Kd	0.55	137	R, 115, S	*Slc37a2*
No. 45	SPGEEMQFL	H-2-Ld	0.55	154	L, 641, F	*Timeless*
No. 46	LYLPMVQSVA	H-2-Kd	0.55	547	A, 75, V	*Dazap2*
No. 47	RPVNLMEV	H-2-Ld	0.6	749	A, 489, P	*Tbc1d19*
No. 48	FPLQGLHKL	H-2-Ld	0.6	23	C, 384, F	*Tbc1d1*
No. 49	LPALASNL	H-2-Ld	0.6	672	P, 572, L	*Zfp467*
No. 50	KPLINRHL	H-2-Ld	0.6	864	Q, 949, K	*Snx19*
No. 51	CGPLKLLVHE	H-2-Dd	0.6	3,255	A, 237, V	*Supv3l1*
No. 52	SPGEEMQF	H-2-Ld	0.6	755	L, 641, F	*Timeless*
No. 53	IPSHYTEL	H-2-Ld	0.6	631	V, 620, I	*Atg2b*
No. 54	HLPRNSAMI	H-2-Dd	0.6	3,499	T, 359, A	*Dcp1a*
No. 55	NPGAAEPPL	H-2-Ld	0.6	586	G, 266, E	*Chd8*
No. 56	SDVNAFNL	H-2-Ld	0.6	1,046	D, 40, N	*Trabd*

No. 57	RAQTQPPNL	H-2-Ld	0.6	1,120	R, 460, P	*Rbm27*

Supplemental Table 3. Tested peptides of neoepitopes predicted in CMS5a cells.

Peptide ID	Peptide sequence	IEDB analysis			Substitution (wild type, amino acid number, mutation)	Gene
		MHC allele	Percentile rank	ANN IC50		
No. 1	RPIQKATL	H-2-Ld	0.5	423	R, 289, P	*Pex26*
No. 2	LNPHAPEF	H-2-Ld	0.3	236	Q, 86, H	*Usp10*
No. 3	NPHAPEFI	H-2-Dd	0.8	6,067	Q, 86, H	*Usp10*
No. 4	SSPRQSAA	H-2-Dd	0.7	5,389	G, 429, R	*Nlrc5*
No. 5	MPPDRSHC	H-2-Dd	0.9	6,322	C, 774, S	*Malt1*
No. 6	HYPKREKV	H-2-Dd	0.7	5,738	D, 119, Y	*Thumpd2*
No. 7	WSPVTSTL	H-2-Dd	0.4	3,089	A, 324, T	*Dctn2*
No. 8	QGPPDCQV	H-2-Dd	0.3	2,679	W, 401, C	*Maged1*
No. 9	GPPDCQVP	H-2-Dd	0.4	3,229	W, 401, C	*Maged1*
No. 10	PPPTALNV	H-2-Dd	0.8	5,949	G, 178, V	*Sec24d*
No. 11	CGPLKLLV	H-2-Dd	0.2	1,399	A, 237, V	*Supv3l1*
No. 12	VSFVAFYI	H-2-Ld	0.9	2,080	I, 1230, F	*Smc4*
No. 13	LPSGCHGV	H-2-Ld	0.9	2,095	G, 869, C	*Pprc1*
No. 14	STPGHENF	H-2-Dd	0.5	3,875	G, 681, S	*Mark2*

No. 15	SPESPLSF	H-2-Ld	0.4	335	R, 936, P	*Ganab*
No. 16	FMPKMDII	H-2-Dd	0.3	1,836	V, 434, F	*Alas1*
No. 17	SGPSSSKL	H-2-Dd	0.1	479	A, 115, S	*Ccdc21*
No. 18	PGPGTEAL	H-2-Dd	0.2	817	R, 682, T	*Ehmt2*
No. 19	QLPCNGVL	H-2-Dd	0.7	5,377	R, 693, P	*Myh9*
No. 20	TPPRLLST	H-2-Dd	0.7	5,426	R, 696, P	*Rnf123*
No. 21	LLPDNRHY	H-2-Dd	0.9	6,454	A, 350, P	*Alg10b*
No. 22	LPQPAHLQ	H-2-Ld	0.7	1,244	V, 35, L	*Tlcd1*
No. 23	ALHSSAQL	H-2-Kd	0.85	4,681	V, 421, A	*Zfp326*
No. 24	TPYNMVPI	H-2-Ld	0.3	225	V, 2389, I	*Hivep1*
No. 25	VPIGGIHV	H-2-Ld	0.3	168	V, 2389, I	*Hivep1*
No. 26	TPCAFGDL	H-2-Ld	0.1	24	R, 129, L	*Dus3l*
No. 27	TGGETQIF	H-2-Dd	0.3	2,029	L, 59, F	*Wdr74*
No. 28	FSPNPYWL	H-2-Dd	0.3	2,160	R, 245, P	*Gnb2l1*
No. 29	WDPKPITL	H-2-Ld	0.2	66	V, 687, L	*Dopey2*
No. 30	KPITLPQF	H-2-Dd	0.7	5,550	V, 687, L	*Dopey2*
No. 31	LPQFKQML	H-2-Ld	0.9	2,319	V, 687, L	*Dopey2*
No. 32	GGPSMRNT	H-2-Dd	0.2	1,547	R, 176, S	*Stard13*
No. 33	TGGTDGHL	H-2-Dd	0.7	5,569	V, 178, L	*Preb*
No. 34	NPHAPEFIL	H-2-Ld	0.2	114	Q, 86, H	*Usp10*
No. 35	CDPSRVRVL	H-2-Dd	0.6	4282	H, 1361, L	*Flna*

No. 36	LGPGIQSGT	H-2-Dd	0.8	1,218	H, 1361, L	*Flna*
No. 37	MPPDRSHCS	H-2-Dd	0.6	4,356	C, 774, S	*Malt1*
No. 38	CGPLKLLVH	H-2-Dd	0.4	1,423	A, 237, V	*Supv3l1*
No. 39	AYCKQNLEI	H-2-Kd	0.4	144	M, 763, I	*Lztr1*
No. 40	YPLSDLLFL	H-2-Ld	0.45	12	Q, 226, L	*Ccdc97*
No. 41	QYIHSANVL	H-2-Kd	0.3	22	K, 136, Q	*Mapk1*
No. 42	GSPESPLSF	H-2-Dd	0.3	1,871	R, 936, P	*Ganab*
No. 43	SGPSSSKLP	H-2-Dd	0.8	1,268	A, 115, S	*Ccdc21*
No. 44	LPDNRHYTF	H-2-Ld	0.25	53	A, 350, P	*Alg10b*
No. 45	LGASSAMVF	H-2-Dd	0.7	2,949	M, 17, L	*Atp6v0c*
No. 46	LPQPAHLQT	H-2-Ld	0.75	599	V, 35, L	*Tlcd1*
No. 47	QPMSPAPGL	H-2-Ld	0.35	409	A, 49, S	*Eid2b*
No. 48	PKPITLPQF	H-2-Dd	0.9	6,758	V, 687, L	*Dopey2*
No. 49	QVPECTVVF	H-2-Dd	0.6	3,913	G, 314, C	*Klf10*
No. 50	YYSSPAQHV	H-2-Kd	0.3	74	Q, 277, H	*Tor1aip2*
No. 51	AYSEEKSYI	H-2-Kd	0.3	26	T, 192, S	*Zfp472*
No. 52	SSPRQSAALL	H-2-Dd	0.85	6,456	G, 429, R	*Nlrc5*
No. 53	CGPLKLLVHE	H-2-Dd	0.6	3,255	A, 237, V	*Supv3l1*
No. 54	RYVSYGCRKI	H-2-Kd	0.8	612	D, 728, Y	*Mlh3*
No. 55	DGFMPKMDII	H-2-Dd	0.8	8,178	V, 434, F	*Alas1*
No. 56	MTPPRLLSTM	H-2-Dd	0.5	8,358	R, 696, P	*Rnf123*

No. 57	LLPDNRHYTF	H-2-Dd	0.65	6,565	A, 350, P	*Alg10b*
No. 58	VYIPALHSSA	H-2-Kd	0.9	884	V, 421, A	*Zfp326*
No. 59	PHPRRYACSL	H-2-Dd	0.75	11,239	R, 313, L	*Ino80b*
No. 60	SYDSYATHNV	H-2-Kd	0.2	387	E, 172, V	*Cirbp*
No. 61	PYWLCAATGP	H-2-Kd	0.5	2,007	R, 245, P	*Gnb2l1*
No. 62	SYYSSPAQHV	H-2-Kd	0.3	70	Q, 277, H	*Tor1aip2*

Supplemental Table 4. Number of non-synonymous SNVs in transcripts in the tested murine tumors.

Analysis		Number of mutations		
		CT26 cells	CMS7 cells	CMS5a cells
Whole exome sequencing	Sequence data	15,383	11,158	14,579
	Somatic mutations	3,387	2,904	3,188
	Mutations in transcript	1,709	1,423	1,652
	Non-synonymous SNVs	1,099	943	1,126
RNA sequencing	Mutations in expressed genes	285	239	266

Supplemental Table 5. Comparative gene expression analysis of transcription factors associated with M1 and M2 macrophages.

Probe Set ID	Gene Symbol	Log2 fold change (CMS5a/NY vs. CMS5a)	Log2 fold change (Treated CMS5a vs. nontreated CMS5a)
1427418_a_at	*Hif1a*	-0.102006123	0.596742314
1448183_a_at	*Hif1a*	0.52928722	0.999098388
1416035_at	*Hif1a*	-0.204768616	0.546580511
1431981_at	*Hif1a*	0.437446992	0.28195183
1448436_a_at	*Irf1*	1.38574598	0.193030332
1426111_x_at	*Irf3*	-0.13244198	0.12839379
1416898_a_at	*Irf3*	-0.179123813	0.243878575
1438721_a_at	*Irf3*	0.367845221	0.345820299
1435271_at	*Irf3*	-0.51141804	0.320664017
1449678_at	*Irf5*	0.684146931	-0.032628351
1460231_at	*Irf5*	0.186372068	-0.358627819
1427742_a_at	*Klf6*	0.697337524	0.15782681
1418280_at	*Klf6*	0.07351287	-0.141876486
1433508_at	*Klf6*	0.357750848	-0.172162176
1447448_s_at	*Klf6*	0.20465045	-0.22858757
1459718_x_at	*Klf6*	0.312089659	-0.395802287
1421266_s_at	*Nfkbib*	0.545243075	0.216167019
1446718_at	*Nfkbib*	0.799600613	0.095705746
1436074_at	*Nfkbid*	0.585842464	-0.787725321
1420915_at	*Stat1*	0.83066829	0.388993093
1450034_at	*Stat1*	0.803017372	0.372078432
1450033_a_at	*Stat1*	0.893920665	0.102814437
1450259_a_at	*Stat5a*	0.760089916	1.029633909
1422103_a_at	*Stat5b*	0.911950995	0.793369015
1422102_a_at	*Stat5b*	0.573340705	0.514432852
1421174_at	*Irf4*	1.4955416	0.442582036

1421173_at	*Irf4*	1.632703017	0.169193812
1417394_at	*Klf4*	0.879606929	-0.327527681
1417395_at	*Klf4*	0.873058937	-0.494870578
1444073_at	*Maf*	0.627607519	1.374526274
1447945_at	*Maf*	0.629887828	0.757822153
1437473_at	*Maf*	0.209699443	0.132466934
1424942_a_at	*Myc*	-0.177360981	-0.22561396
1420715_a_at	*Pparg*	1.427346999	2.042408332
1426587_a_at	*Stat3*	0.487912725	0.722098759
1460700_at	*Stat3*	0.415510662	0.507682418
1421708_a_at	*Stat6*	0.559017964	0.640321842
1426353_at	*Stat6*	0.272166348	0.10340839